Journal of Crystal Growth 318 (2011) 669–673

Contents lists available at ScienceDirect

Journal of Crystal Growth

journal homepage: www.elsevier.com/locate/jcrysgro

Growth and radiation resistant properties of 2.7–2.8 μm Yb,Er:GSGG laser crystal

Dunlu Sun [a,*], Jianqiao Luo [a], Qingli Zhang [a], Jingzhong Xiao [b], Wenpeng Liu [a], Shangfei Wang [c], Haihe Jiang [a], Shaotang Yin [a]

[a] Anhui Institute of Optics and Fine Mechanics, Chinese Academy of Sciences, Hefei 230031, China
[b] Physics Department, Universidade de Coimbra, Rua Larga, P-3004-516 Coimbra, Portugal
[c] Department of Polymer Science and Engineering, University of Science and Technology of China, Hefei 230026, China

ARTICLE INFO

Available online 27 November 2010

Keywords:
A1. Radiation resistance
A1. Color-center
A2. Single crystal growth
B1. Yb Er:GSGG
B2. Laser material

ABSTRACT

High quality Yb^{3+} and Er^{3+} co-doped $Gd_3Sc_2Ga_3O_{12}$ (Yb,Er:GSGG) crystals were grown by the Czochralski (Cz) method, and their absorption and fluorescence properties with the gamma-ray radiation have been investigated. In comparison with Er:YAG crystals, these co-doped crystals exhibit much less color-center absorption after the illumination of gamma-ray. Excited by 940 nm LD, two of the strongest fluorescence peaks were observed near 2.7 and 2.8 μm, suggesting that the Yb^{3+} can act as a sensitizer for Er^{3+} ion in Yb,Er:GSGG crystals. In particular, the fluorescence intensity of these crystals does not deteriorate by the radiation of gamma-ray even with a dose of 100 Mrad, indicating that Yb,Er:GSGG possesses high capability for enduring the gamma radiation and is a potential laser gain medium for being used under radiant environment.

1. Introduction

It is well known that the solid-state laser will encounter an impact of gamma-ray radiation and high-energy particles in outer space and some harsh radiation environment [1]. Therefore, it is attractive and necessary to develop novel crystals that improve their radiation resistant property for the laser device application under the radiation environment. Recently, a great progress has been achieved in the studies of the radiation effect on the spectra and laser performance of crystals such as Nd:YAG($Y_3Al_5O_{12}$), Nd:GGG($Gd_3Ga_5O_{12}$) and Nd,Cr:GSGG($Gd_3Sc_2Ga_3O_{12}$) [2–4]. For instance, Zharikov et al. reported that Nd,Cr:GSGG laser performance was unaffected by UV or ^{60}Co gamma radiation up to 10 Mrad [2], and the crystal was not damaged even if illuminated by 100 Mrad radiation doses [3]. While in comparison, the laser output of the commonly used Nd:YAG laser was found to deteriorate seriously under the radiation condition, and the output energy dropped by an order of magnitude after 1 Mrad gamma-ray exposure [4]. More recently, the strong radiation resistance properties of single doped Nd:GSGG and Cr:GSGG crystals have also been demonstrated [5,6] and GSGG crystals exhibit better radiation resistant ability than the YAG crystals. In addition, GSGG can be grown easily in large size without an optically inhomogeneous central core [1], which is advantageous to generate high power laser output. These suggest that GSGG crystals have more advantages for the application under radiation environment than YAG crystals.

Lasers based on the trivalent erbium 3 μm transition ($^4I_{11/2} \rightarrow {}^4I_{13/2}$) can be utilized for medical applications and can act as pumping sources for infrared optical parametric oscillators. Er^{3+} doped GSGG crystal is expected to become such a radiation resistant material that can be applied under the radiation environment. Stoneman and Esterowitz have reported the 2.8 μm Er^{3+}:GSGG laser pumped by a Ti:sapphire laser tuned to 970 nm [7]. It is well known that all-solid-state laser systems pumped with laser diode (LD) permit a high pumping efficiency and compact setup, without the high consumption of electrical energy and the requirement for cooling system [8]. However, single doped Er^{3+} crystal has a principal drawback of low absorption cross-section in laser diodes emission range (0.9–1.0 μm), which limits the pump efficiency. To solve this problem, a key approach is co-doping a second ion as a sensitizer for Er^{3+}. Yb^{3+} is an ideal candidate to play this role, since its high absorption cross-section and broad absorption band can offer excitation tuning in the wavelength region of 875–1000 nm, in which the large overlap between Yb^{3+} emission and Er^{3+} absorption can allow resonant energy transfer from Yb^{3+} to Er^{3+} [9].

Therefore in this work, we performed the Czochralski growth of Yb,Er:GSGG crystals, and investigated the influence of gamma radiation with different doses on the absorption and fluorescence spectra. The mechanism of luminescence and radiation resistance of Yb,Er:GSGG crystal are also analyzed and discussed.

* Corresponding author. Tel./fax: +86 551 5591039.
E-mail address: dlsun@aiofm.ac.cn (D. Sun).

0022-0248/$ - see front matter © 2010 Elsevier B.V. All rights reserved.
doi:10.1016/j.jcrysgro.2010.11.118

2. Experimental

Yb,Er:GSGG crystals were grown by the Czochralski method using a SJ78-3 furnace and an automatic diameter controlled (ADC) growth system. The Gd_2O_3, Ga_2O_3 and Sc_2O_3 powders with the purity of 99.99% and Yb_2O_3, Er_2O_3 with 99.999% were used as raw materials and weighed according to the designed compositions; the Ga_2O_3 was overweighed by 2 wt% in order to compensate its evaporation loss during the growth. After being mixed thoroughly and pressed into disks, the polycrystalline raw materials were synthesized and loaded into an iridium crucible. The crystal was grown using ⟨1 1 1⟩-oriented GSGG seeds and in a chamber atmosphere of nitrogen (98%) and oxygen (2%). The pulling and rotation rate were optimized to 1–2 mm/h and 10–20 rpm, respectively. Samples were cut from the post-annealing crystals perpendicular to the growth direction and polished on both sides to 3 mm in thickness. The concentrations of Yb^{3+} and Er^{3+} ions in the grown crystal were measured using inductively coupled plasma atomic emission spectrometry (ICP-AES). The segregation coefficient K is calculated as the ratio of the rare earth mole fraction in the crystal to the melt. Crystal structure was identified by X-ray diffractometer (Philips PW 3710) using Cu Kα radiation.

The samples were radiated by a ^{60}Co gamma-ray source with the dose rate of 82 Gy/min, radiation times of 100 and 200 h at room temperature, corresponding to the doses of about 50 and 100 Mrad, respectively. The absorption spectra were recorded using a PE lambda 900 spectrophotometer. A Fourier transform infrared (FTIR) spectrometer was used to measure the fluorescence spectra, with an exciting source of 940 nm LD. In order to obtain accurate comparison, the absorption and luminescence measurements under gamma radiation were performed using the same samples and under the same conditions.

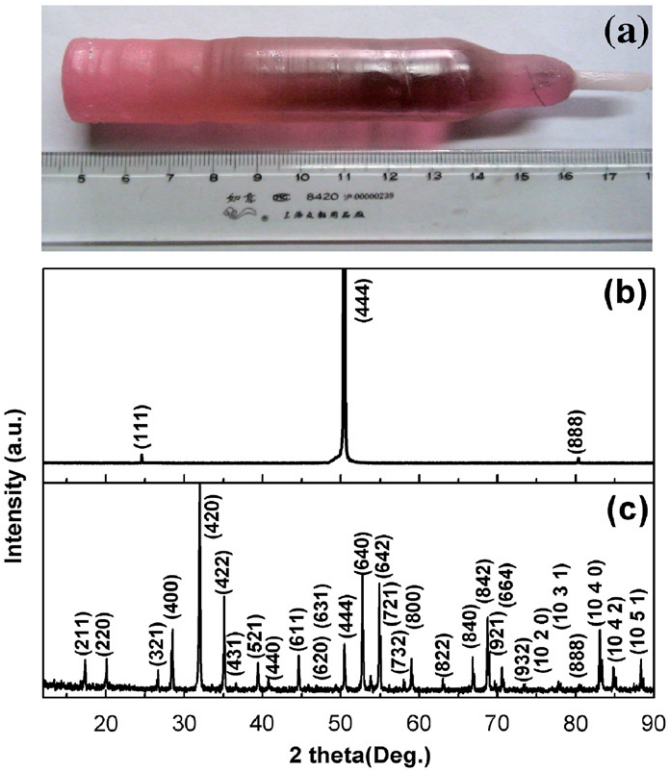

Fig. 1. (a) Photograph of the as-grown Yb,Er:GSGG laser crystal; (b) XRD diffraction pattern of Yb,Er:GSGG crystal along the ⟨1 1 1⟩ direction; (c) the powder XRD diffraction pattern of Yb,Er:GSGG crystal.

3. Results and discussion

A photograph of the as-grown Yb,Er:GSGG laser crystal is shown in Fig. 1(a). The crystal is free of scattering and cracking with a dimension of ∅26 mm × 90 mm. The Yb^{3+} and Er^{3+} ions concentrations in the grown crystals were determined to be 9.6 and 30.75 at% by the ICP-AES method, respectively. Thus the segregation coefficients of Yb^{3+} and Er^{3+} ions were calculated approximately to be 0.96 and 0.88, respectively, after the initial 10 at% Yb^{3+} and 35 at% Er^{3+} ions in the melt were taken into account.

The XRD patterns of the polished (1 1 1) crystal slice and the powders are shown in Fig. 1(b) and (c), respectively. Only the (l l l) reflections appeared in the crystal slice diffraction pattern and all observed reflections were indexed into the powder diffraction pattern, indicating that the crystal has pure phase and good crystalline quality. $Gd_3Ga_3Sc_2O_{12}$(GSGG) crystallizes in garnet structure with a cubic space group symmetry I_{a3d} (no. 230; Z=8). In Yb,Er:GSGG crystal, both Yb^{3+} and Er^{3+} ions occupy the Gd^{3+} sites of dodecahedral (D_2 symmetry) in the cubic GSGG lattice. The lattice parameter of the Yb,Er:GSGG was determined to be a=12.5187 Å, which is slightly smaller than that of the pure GSGG crystal (a_0=12.5588 Å) [10], as both the ionic radii of Yb^{3+} and Er^{3+} are smaller than that of Gd^{3+}.

The absorption spectra of Er:GSGG and Yb,Er:GSGG crystals before gamma-ray radiation are shown in Fig. 2. The absorption spectrum of Er:GSGG crystal consists of ten absorption bands centered at around 407, 442, 452, 490, 520, 546, 654, 803, 972 and 1500 nm, which correspond to the transitions from $^4I_{15/2}$ to $^4G_{11/2}$, $^2H_{9/2}$, $^4F_{5/2}$, $^4F_{7/2}$, $^2H_{11/2}$, $^4S_{3/2}$, $^4F_{9/2}$, $^4I_{9/2}$, $^4I_{11/2}$ and $^4I_{13/2}$, respectively. The absorption band of Yb^{3+} is located in the range of 875–1000 nm [9], corresponding to the translation of $^2F_{7/2}\rightarrow{}^2F_{5/2}$ levels. Therefore the absorption band of Yb,Er:GSGG crystal in the

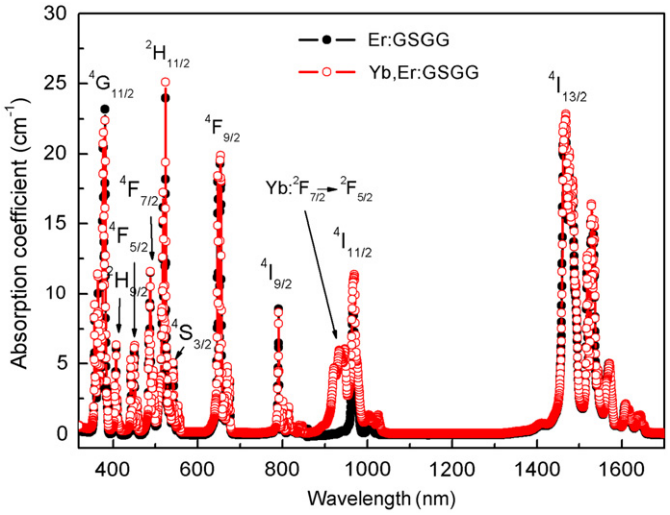

Fig. 2. Absorption spectra of Er:GSGG and Yb,Er:GSGG crystals.

range of 875–1000 nm is expected to be consisted of the translations of $^2F_{7/2}\rightarrow{}^2F_{5/2}$ of Yb^{3+} ions and $^4I_{15/2}\rightarrow{}^4I_{11/2}$ of Er^{3+} ions. The increased absorption coefficient and boarded absorption band of Yb,Er:GSGG crystal are quite suitable for the currently well developed 940–980 nm LD pump source. Especially, there is a large absorption coefficient (5.5 cm^{-1}) and wide absorption band (FWHM ~ 30 nm) at 940 nm due to the doping of Yb^{3+} ions in Yb,Er:GSGG crystal, which allows the crystal to be pumped by a 940 nm LD for the possibility of generating laser output. While in comparison, the absorption near 940 nm of the single doped Er:GSGG crystal is too weak to be pumped by a 940 nm LD.

The fluorescence spectrum of Yb,Er:GSGG crystal excited by 940 nm LD is shown in Fig. 3. Two of the strongest peaks near 2.7 and 2.8 μm indicate that the Yb^{3+} can act as a sensitizer for Er^{3+} ions. In addition, many fluorescence peaks appearing in the measured wavelength range of 2.6–3.0 μm can be assigned to the transitions of stark sub-levels between the $^4I_{11/2}$ and $^4I_{13/2}$, which could be possibly derived by measuring the absorption and fluorescence spectra in a low-temperature environment. For example in Er:YAG, the stark sub-levels of $^4I_{11/2}$ at 6766, 6858 and 6949 cm^{-1} and $^4I_{13/2}$ at 10 252, 10 281, 10 360, 10 370 and 10 411 cm^{-1} have been obtained at 4.2 K [11]. Fig. 4 shows the schematic diagram of major up-conversion and cross-relaxation processes responsible for the formation of inverse population for 2.7 or 2.8 μm radiation translation in Yb,Er:GSGG crystal with high Er^{3+} ions concentration. For sake of simplicity, we shall neglect the up-conversion from $^4S_{3/2}$, responsible for violet and blue emission from high-energy levels of $^2P_{3/2}$ and $(^4F, ^2G1)_{9/2}$[12]. The absorbed energy can be transferred from $^2F_{5/2}$ of Yb^{3+} to the $^4I_{11/2}$ of Er^{3+}, as these two energy levels are very close. However unavoidably, part of the energy of Er^{3+} will return to Yb^{3+} ions, which generates the emission near 1 μm. Absorbed energy of $^4I_{13/2}$ level will be transfered to $^4I_{11/2}$ by non-radiation transition and generates weak 2.7–3 μm emission. The following energy transfer from $^4I_{13/2}$ to $^4I_{15/2}$ near 1.5 μm will be predominant under the condition of low doped Er^{3+} concentration [13–15] (about 0.5–2.0 at%). In general, since the lifetime of upper laser level $^4I_{11/2}$ is smaller ($\tau_1 \sim 0.1$–1.6 ms depending on the different martix, such as YAG, YSGG, GGG, GSGG, etc.) than that of lower laser level $^4I_{13/2}$ ($\tau_2 \sim 3$–8 ms) [16], it is difficult to obtain 2.7–3 μm laser output from the transition of $^4I_{11/2} \rightarrow {}^4I_{13/2}$. However, with highly doped Er^{3+} ions (> 30 at%), an up-conversion mechanism $(^4I_{13/2} \rightarrow {}^4I_{15/2}) + (^4I_{13/2} \rightarrow {}^4I_{9/2} \sim\sim\sim\rangle {}^4I_{11/2})$ and a three-ion cross-relaxation mechanism involving $^4S_{3/2}$ level $(^4S_{3/2}(^2H_{11/2}) \rightarrow {}^4I_{15/2}) + (^4I_{15/2} \rightarrow {}^4I_{13/2}) + (^4I_{15/2} \rightarrow {}^4I_{9/2} \sim\sim\sim\rangle {}^4I_{11/2})$ have been proposed to overcome this "bottleneck", as shown in Fig. 4(b) and (d), respectively. ($\sim\sim\sim\rangle$means multi-phonon transition process). Both the two mechanisms influence the population inversion; they produce an even population of the initial ($^4I_{11/2}$) and final ($^4I_{13/2}$) energy level as a whole. In addition, it should be pointed out that another up-conversion process $(^4I_{11/2} \rightarrow {}^4I_{15/2}) + (^4I_{11/2} \rightarrow {}^4F_{7/2})$, as shown in Fig. 4(c), followed by the multiphonon transitions to $^4S_{3/2}$, will generate green and red emission and deactivate the initial laser level, but this negative effect can be compensated by the mentioned cross-relaxation mechanism involving $^4S_{3/2}$[17].

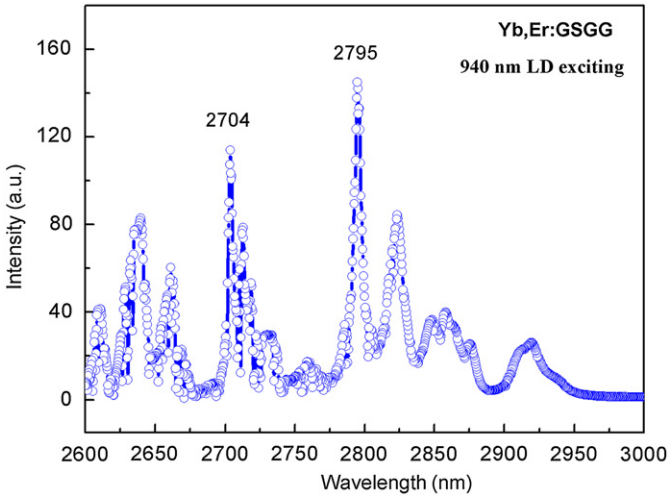

Fig. 3. Fluorescence spectrum of Yb,Er:GSGG crystal excited by 940 nm LD.

The transmission spectra of Er:YAG crystal before and after gamma-ray radiation are shown in Fig. 5(a). The gamma radiation has little influence on the transmission of Er:YAG crystal in the wavelength range above 900 nm. However, below 900 nm, the transmission of Er:YAG crystal shows a considerable decrease after 50 or 100 Mrad gamma radiation, resulting from a lot of color-center absorption in Er:YAG crystal. The transmission spectra of Yb,Er:GSGG crystal before and after gamma-ray radiation are shown in Fig. 5(b). The gamma radiation has almost no influence on the transmission of Yb,Er:GSGG crystal in the wavelength range above 600 nm, especially in the assumed laser region of 2.6–3.0 μm. In comparison with the non-radiated one (not shown), transmissions of radiated sample are unchanged within experimental uncertainty. In addition, below 600 nm, as compared with Er:YAG, the transmission of Yb,Er:GSGG crystals shows a slight decrease after gamma radiation, suggesting that only a small amount color-center absorption was formed in Yb,Er:GSGG crystal. This phenomenon can be interpreted base on the theoretical calculation carried out by Xu et al. [18]. In GSGG crystal, the Sc atom at the octahedral site shows a stronger covalent characteristic and an increased bond order in comparison with Ga or Al at the same sites in GGG or YAG crystals, which may enhance the ability of color-center formation resistance in GSGG crystal. In addition, it is

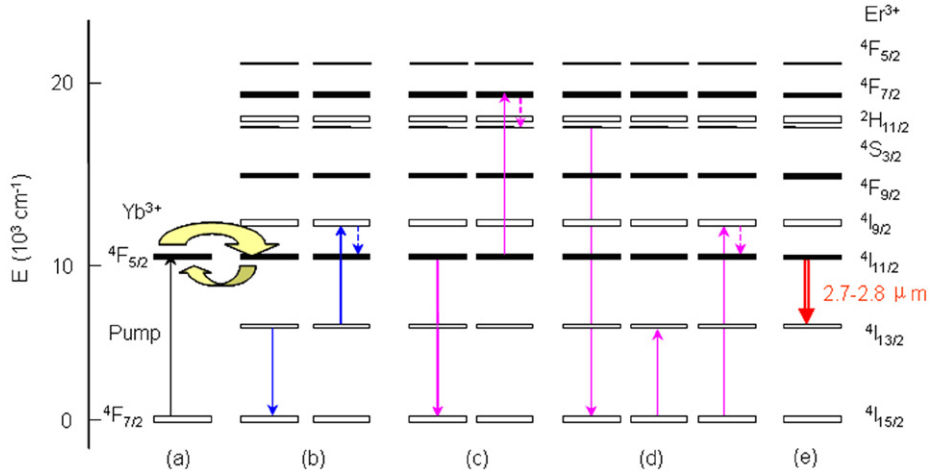

Fig. 4. Schematic diagram of main up-conversion and cross-relaxation processes responsible for the formation of inverse population for 2.7 or 2.8 μm fluorescence in Yb,Er:GSGG crystal with high Er^{3+} ions concentration. Wave arrows indicate multiphonon translations. (a) pumping; (b) up-conversion from $^4I_{13/2}$; (c) up-conversion from $^4I_{11/2}$; (d) three ions cross-relaxation of $^4S_{3/2}$ level; (e) 2.7–2.8 μm emission regimes.

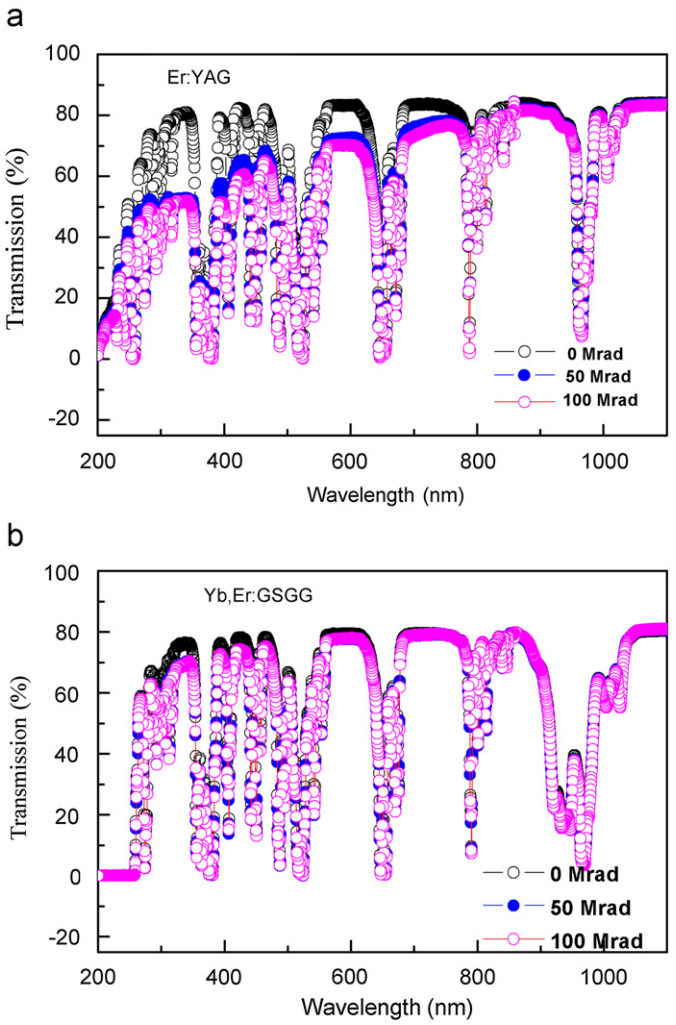

Fig. 5. (a) Transmission spectra of Er:YAG crystal before and after gamma-ray radiation; (b) Transmission spectra of Yb,Er:GSGG crystal before and after gamma-ray radiation.

also noted that the transmission of Yb,Er:GSGG crystal irradiated by 100 Mrad is close to the 50 Mrad irradiated one, which indicates that the 50 Mard doses may be a saturation radiation value. Accordingly, Er:YAG crystal exhibits a more evident decrease in transmission than the Yb,Er:GSGG crystal, indicating that Yb,Er:GSGG crystal possesses superior radiation resistant performance than Er:YAG crystal.

The fluorescence spectra of Yb,Er:GSGG crystal excited by 940 nm LD before and after gamma-ray radiation are shown in Fig. 6. It can be noted that the fluorescence intensity is not influenced by the gamma radiation with 50 Mrad, and it only shows a slight decrease after the gamma radiation of 100 Mrad, which suggests that the Yb,Er:GSGG crystal can resist strong gamma radiation. Matkovski et al. [19,20] proposed that the radiation-stimulated changes of the garnet crystal properties were associated with two main processes: ionizing recharging of growth defects and formation of radiation defects through the impact mechanism, through which the formed color-center can absorb pumping light as well as reabsorb laser radiation, even though trifling color-center absorption in assumed laser region will generate a disastrous influence on the laser performance of crystal [4]. Therefore, a tiny color-center absorption may be considered to lead to the slight decrease in the fluorescence intensity of Yb,Er:GSGG crystal after the 100 Mrad gamma radiation. But the fluorescence property of Yb,Er:GSGG crystal was not seriously deteriorated even

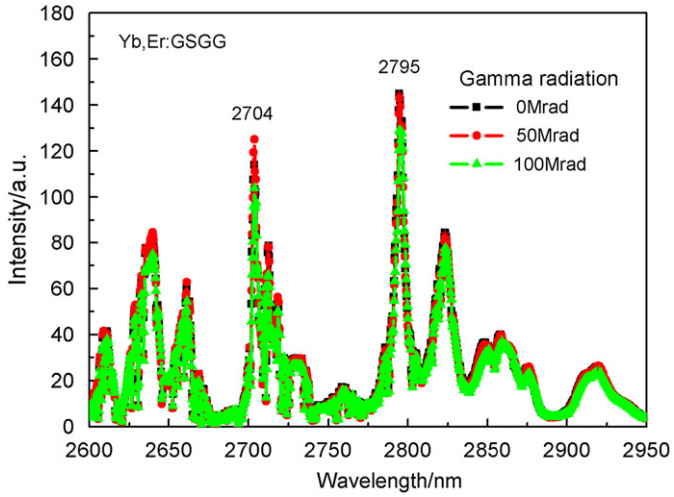

Fig. 6. Fluorescence spectra of Yb,Er:GSGG crystal excited by 940 nm LD before and after gamma-ray radiation.

with 100 Mrad gamma radiation doses, indicating that the crystals exhibit excellent radiation resistant ability.

4. Conclusions

The effects of gamma-ray radiation on the absorption and luminescence properties of Yb,Er:GSGG crystals have been investigated. In comparison with the widely applied YAG-based laser crystals, only small amount of color-center absorption was observed in Yb,Er:GSGG. In addition, the fluorescence result of Yb,Er:GSGG suggests that Yb^{3+} can act as a sensitizer for Er^{3+} ion and the 2.7–2.8 μm laser output may be generated by 940 nm LD pumping. In particular, the fluorescence intensity of Yb,Er:GSGG crystal was not influenced by the radiation of 50 Mrad and also did not deteriorate even by the radiation of 100 Mrad gamma ray. Therefore, Yb,Er:GSGG crystal has excellent ability of radiation resistance and is a potential candidate for a laser gain medium that can be used under radiant environments such as outer space.

Acknowledgments

We thank T.S. Zhang and R.F. Kan for the assistance in the infrared spectra measurement. This work was financially supported by the Knowledge Innovation Program of the Chinese Academy of Sciences and National Nature and Science Foundation of China (nos. 50872135,50772112 and 90922003).

References

[1] S.E. Stokowski, M.H. Randles, R.C. Morris, IEEE J. Quantum Electron. 24 (1988) 934.
[2] E.V. Zharikov, I.I. Kuratev, V.V. Laptev, S.P. Naselskii, A.I. Ryabov, G.N. Toropkin, A.V. Shestakov, I.A. Shcherbakov, Bull. Acad. Sci. USSR Phys. Ser. 48 (1984) 103.
[3] K. Yu., E.V. Danileko, V.V. Zharikov, Yu.P. Laptcv, V.N. Minaev, A.V. Nikolaev, A.V. Nikolaev, G.N. Sidorin, I.A. Toropkin, Sov. Shcherbakov, J. Quantum Electron. 15 (1985) 286.
[4] D. Sugak, A. Matkovskii, A. Durygin, A. Suchocki, I. Solskii, S. Ubizskii, K. Kopczynski, Z. Mierczyk, P. Potera, J. Lumin. 82 (1999) 9.
[5] D.L. Sun, J.Q. Luo, J.Z. Xiao, Q.L. Zhang, H.H. Jiang, S.T. Yin, Y.F. Wang, X.W. Ge, Appl. Phys. B 92 (2008) 529.
[6] Jianqiao Dunlu Sun, Qingli Luo, Jingzhong Zhang, Jiayue Xiao, Haihe Xu, Shaotang Yin Jiang, J. Lumin. 128 (2008) 1886.
[7] R.C. Stoneman, L. Esterowitz, Opt. Lett. 17 (1992) 816.
[8] T. Jensen, A. Diening, G. Huber, Opt. Lett. 21 (1996) 585.
[9] E. Cantelar, J.A. Muñoz, J.A. Sanz-García, F. Cusso, J. Phys. Condens. Matter 10 (1998) 8893.

[10] S. Yamazaki, F. Marumo, K. Tanaka, H. Morikawa, N. Kodama, K. Kitamura, Y. Miyazawa, J. Solid State Chem. 108 (1994) 94.
[11] J.A. Koningstein, J.E. Geusic., Phys. Rev. 136A (1964) 726.
[12] I. Ursu, V. Lupei, S. Georgescu, C. Ionescu, in: Proceedings of the Second International Conference on Trends in Quantum Electronics, Bucharest, Romania, September CIP, 1985, pp. 38–39.
[13] B. Denker, B. Galagan, V. Osiko, S. Sverchkov, A.M. Balbashov, J.E. Hellström, V. Pasiskevicius, F. Laurell, Opt. Commun. 271 (2007) 142.
[14] J.H. Huang, Y.J. Chen, X.H. Gong, Y.F. Lin, Z.D. Luo, Y.D. Huang, Appl. Phys. B 97 (2009) 431.
[15] W.X. You, Y.F. Lin, Y.J. Chen, Z.D. Luo, Y.D. Huang, Opt. Mater. 29 (2007) 488.
[16] Bradley J. Dinerman, F.Moulton Peter, 3 μm cw laser operations in erbium-doped YSGG, GGG, and YAG, Opt. Lett. 19 (1994) 1143.
[17] V. Lupei, S. Georgescu, V. Florea, IEEE J. Quantum Electron. 29 (1993) 426.
[18] Y.N. Xu, W.Y. Ching, B.K. Brickeen, Phys. Rev. B 61 (2000) 1817.
[19] A. Matkovski, D. Sugak, S. Ubizski, I. Kityk, Radiat. Eff. Defect. Solids 133 (1995) 153.
[20] A. Matkovskii, P. potera, D. Sugak, L. Grigorjeva, D. Millers, V. Pankratov, A. Suchocki, Cryst. Res. Technol. 39 (2004) 788.